



# Assessment of the Critical State Locus in Reconstituted Samples and Calibration of NorSand Model

Rios Villarreal Eliza Alejandra<sup>(✉)</sup> and Botero Jaramillo Eduardo

Universidad Nacional Autónoma de México, Mexico City, Mexico  
eliza.rios.villa@comunidad.unam.mx

**Abstract.** The critical state theory has been widely applied in geotechnics, and understanding the mechanical and geotechnical properties of particulate materials is one of the major challenges nowadays. In the mining industry, this is a concern regarding tailings storage facilities, that experience transitions from drained to undrained conditions, which might trigger phenomena like static liquefaction compromising the stability of the impoundment; the seeking of constitutive models that allow doing the behavior analysis of tailings and evaluate the global stability of TSF must lead to use models based on the critical state theory. The present research explores experimentally the assessment of the critical state locus in reconstituted samples of iron tailings, through drained (CID) and undrained (CIU) triaxial tests to evaluate the effectiveness of modeling the behavior of this material using NorSand a critical state model. Once the CSL was defined, several simulations of the tests were done using visual basic coding and comparing the experimental data against the synthetic tests. The testing procedure as well as the results and calibration of the model are discussed.

**Keywords:** Tailings · Critical State Locus · NorSand · laboratory tests

## 1 Introduction

Liquefaction has been the topic of extensive geotechnical engineering research over the past 50 years. To evaluate the response of structures constructed with or on sandy soils, it is important to understand the soil behavior as in situ and under appropriate loading conditions.

According to Seed and Idriss (1983) liquefaction is defined as the condition where effective stresses approach to zero due to undrained cyclic loading. Also under monotonic undrained loading, loose sand can reach peak resistance and then rapidly soften to a condition with constant resistance termed as a steady state (Castro 1969).

Several authors (Been and Jefferies 1985; Roscoe et al. 1958) have reported that large strain behavior of soil can be expressed in terms of its initial in situ state, relative to the steady state line at the same stress level. Steady state is the state parameter that measures how faster dilatation or contraction will happen until the critical state is reached. This parameter is a normalization of data and it is a fundamental parameter for soil constitutive

models which have properties that are invariant with soil density and stress level (Jefferies and Been 2016).

The critical state locus (CSL) theory is widely applied for flow liquefaction, assessment of stress-dilatancy analyses and characterization of mine tailings (Fonseca et al. 2021), in this study given the premise of the state parameter approach that soil behavior under shear loading is primarily a function of its state, a full constitutive model is calibrated to predict the occurrence of liquefaction and subsequently the evolution of pore pressures and strains induced by the phenomenon.

## 2 NorSand Model

### 2.1 Description

The constitutive model “NorSand” is based on plasticity theory and critical state soil mechanics for particulate materials; the approach is to anchor everything to the state parameter to model dense and loose materials; it can simulate softening behavior due the pore pressure increase, of loose soils in undrained conditions (Jefferies and Been 2016).

The model is comprised out of elasticity and plasticity, a yield surface, a flow rule, and hardening/softening rule. Besides uses two axioms according to Been and Jefferies:

- Axiom 1: An unique locus, called the critical state locus (CSL), exists in  $q, p, e$  space such that soil can be deformed without limit at constant stress and constant void ratio.
- Axiom 2: The CSL forms the ultimate condition of all distortional processes in soil, so that all monotonic distortional stress state paths tend to this locus.

It is important to notice two conditions in the definition, the soil is at constant void ratio and has no propensity to change from this constant void ratio condition.

Eight parameters are needed for the calibration of this model, two parameters to define the reference CSL ( $\lambda, \Gamma$ ) see Eq. (1), four parameters to define the plastic behavior ( $\chi_{tc}, N, M, H$ ), and two parameters to define the elastic behavior ( $I_r, \nu$ ) (Jefferies and Been 2016).

$$e_c = \Gamma - \lambda \ln(p_c) \quad (1)$$

where  $\Gamma$  and  $\lambda$  are intrinsic soil properties, meaning that they are not affected by fabric, stress history and density. The subscript “c” denotes critical state conditions,  $\lambda$  is log base 10 and  $\Gamma$  has an associated stress level, which is  $p = 1$  kPa by convention.

The plastic behavior is described through four parameters, the first one  $\chi_{tc}$  represents the relationship between dilatation and state parameter (Been and Jefferies 1985) this soil property is defined under drained triaxial compression, and represented by a state-dilatancy law:

$$D_{min} = \chi_{tc} \psi \quad (2)$$

$T_c$  represents triaxial compression. Plotting  $D_{min}$  versus  $\Psi$  from drained triaxial tests allows to obtain the slope of the trend which is  $\chi_{tc}$ , a detailed procedure of this data

processing is presented in “Soil Liquefaction a Critical State Approach” (Jefferies and Been 2016). The second parameter  $N$ , is the volumetric coupling coefficient for inelastic stored energy (Jefferies and Been 2016) and was formulated by Nova (Nova 1982), pairs with the critical friction ratio  $M$ , and represents the slope of a trend through data, when work flow is considered  $N$  represents a volumetric coupling between mean and distortional strains, is the proportion of work going to volumetric, rather than distortional strain.

Finally,  $H$ , is the hardening parameter, a model soil property, ideally is a constant, but in principle could also be a function of  $\Psi$  (Jefferies and Been 2016). Is determined by calibration of the model to experimental data. Isotropic elasticity in NorSand is adopted in its basic form through shear rigidity  $I_r$  and a constant Poisson’s ratio (Eq. 2)

Further interpretations need to be done to obtain the plastic parameters: plotting  $\eta$  vs  $D^p$  and  $D^p$  versus  $\Psi$ .

Since isotropic plasticity is adopted in NorSand, the dimensionless shear and bulk modulus are written as (Woudstra 2021):

$$I_r = \frac{G}{p} \frac{K}{p} = \frac{1+e}{\kappa} = I_r \frac{2(1+\nu)}{3(1-2\nu)} \quad (3)$$

where  $I_r$  is the shear rigidity, and the shear modulus  $G$  is called  $G_{max}$  in engineering practices, which is often measured during site investigation. Poisson ratio is rarely measured but is generally taken in the range  $0.15 < \nu < 0.25$  without testing.

### 3 Application to a Case Study

#### 3.1 Material

The tailings sample studied is from a tailing’s storage facility located in Colima, Mexico, with specific gravity of 3.14 The grain size distribution was determined using the wet sieve analysis, the fine content is 35% with liquid limit of 21.22% and plasticity index of 6.21%, according to the unified soil classification system (U.S. Department of the Interior Bureau of Reclamation 1999) it’s a low plasticity silt.

#### 3.2 Equipment

Two different triaxial apparatuses were used for laboratory testing (TA-1 and TA-3, see Fig. 1) in both, the axial loading is applied through a system of tension wires which was conceived and applied by Raul J Marsal in 1965, during the design of a triaxial chamber to evaluate strength of rockfill. The main difference between those triaxial equipment, is that one has a transducer to measure the volumetric change (TA-3) and the other has a graduated burette (TA-1) see Fig. 1.

Nevertheless, both has LVDT transducers, load cells specifically TA-3 with submersible load cell, confinement, and back pressure transducers.

Furthermore, oversized lubricated end platens were implemented to reduce the stress concentration due to the friction between soil specimen and the platens restraint. This yields an uniform stress -strain behavior and reliable volume change or pore pressure



**Fig. 1.** Dry talings sample

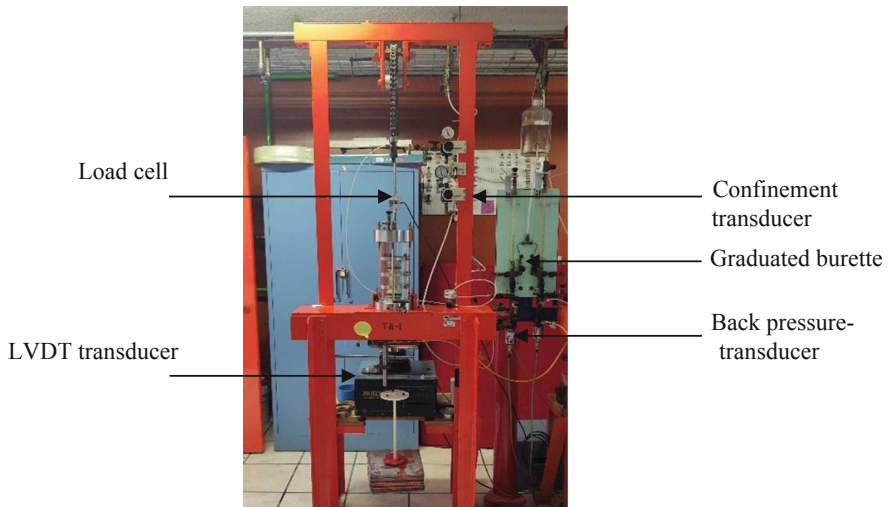


**Fig. 2.** Triaxial chamber TA-1

response (Fonseca et al. 2021). The lubricated end platens comprise a very stiff and smooth platen and two discs of standard triaxial latex membrane; this includes a thin layer of silicone grease between the two latex discs and the surface platen (Rowe and Barden 1964). The silicone grease was applied carefully to avoid interference with the sample drainage.

### 3.3 Experimental Program

#### 3.3.1 Testing Procedure

The limitations for obtaining undisturbed high-quality samples of cohesionless soils is a challenge in geotechnical engineering, due to the sample disturbance during sampling

and handling procedures which may affect the mechanical response of the soil. The ideal method of remolding samples has been an ongoing debate. The moist tamping technique has been widely used in the critical state approach and can produce void ratios looser than the ones in-situ but also might affect the behavior of soil, making it prone to liquefaction due to their metastable honeycomb structure (Fonseca et al. 2021) and there are other options like water sedimentation, slurry deposition that are capable of replicating similar fabric as in situ but requires specific equipment and may induce anisotropy or tendency to dilative behavior. Choosing a remolding method determines the structure of the soil but as the sample reaches the CSL the initial structure is destroyed because of large strains. As this paper deals with cohesionless soils it was considered that the moist tamping technique was able to produce the widest void ratio range, including loose to very loose conditions as well as dense samples.

With this remolding method the sample was assembled by depositing and tamping damp material through ten layers, with a gravimetric water content of 5% for loose samples and dry material for dense ones.

After compacting all layers, the upper filter paper and the latex membrane was placed, and the sample's membrane was attached to the top cap using two O-rings therefore the mold could be removed applying vacuum ( $\approx 10$  kPa) to the soil specimen through the drainage lines to help the sample to keep its shape and density. At this point, the triaxial cell was filled with de-aired water, and cell pressure of 10 kPa was applied to remove the vacuum.

The sample saturation is fundamental to provide reliable values of pore water pressure and volume change during testing. This procedure was conducted in three stages:

- Carbon dioxide method: Flushing  $\text{CO}_2$  through the sample was done for 60 min with low pressure from the bottom drainage line, forcing the air to circulate upwards in the soil specimen through a tube connected to the upper drainage line, which was open and submerged under water, allowing to monitor the bubbling velocity.
- Water flushing:  $160 \text{ cm}^3$  of de-aired water was circulated through percolation under pressure, maintaining the effective confinement of 10 kPa.
- Backpressure increment: The backpressure was gradually increased to high values keeping a low effective stress (approximately of 8 kPa)

Finally, the degree of saturation was determined measuring the por pressure coefficient  $B$  defined by Skempton parameter, obtaining values upon 0.96.

The consolidation phase was carried out varying the mean stress between 30 and 450 kPa to finally load the specimens to failure increasing the axial deformation while keeping the cell pressure constant.

The experimental program was divided in undrained (CIU) and drained (CID) conditions and three types of tests, A loose samples under undrained conditions and B, C both under drained conditions but divided in loose samples (B) and dense samples (C), eight triaxial tests were done:

- Type A: Two CIU tests in loose samples were done in TA-1.

**Table 1.** Final values of triaxial tests

Test	Shearing conditions	p'₀	e₀*
		kPa	(-)
T-1	Drained	30.2	0.567
T-2	Drained	49.13	0.560
T-3	Drained	347.05	0.625
T-4	Drained	450.12	0.546
T-5	Undrained	145.92	0.757
T-6	Undrained	194.36	0.706

\*Void ratio post-consolidation

- Type B: Two CID tests in loose samples were done in TA-3.
- Type C: Two CID tests in dense samples were done in TA-3

All tests followed the procedure mentioned before, with the same preparation method, saturation process consolidation and failure. It is important to mention that before triaxial tests were completed, several compaction tests were done to define the gravimetric water content to use and estimate the void ratios that could be achieved with the remolded technique chosen. In Table 1 there are the characteristics of the triaxial tests done. It is important to mention that even though the void ratios are similar between the samples, specifically between T-1, T-2 and T-4 the behavior is directly affected by the mean effective stress, the dense samples (T-1 and T-2) showed dilative behavior because p' was small enough to allow the volume increase during the failure, meanwhile T-4 was tested at the maximum capability of the equipment in order to reach a high mean effective stress and develop contractive behavior.

### 3.4 Results and Calibration of NorSand

NorSand constitutive model was calibrated using the triaxial test data (CID and CIU). A summary of the calibrated parameters is shown in Table 2.

Details of the calibration are shown in Fig. 2 where two representations of the CSL were done, the first one is a straight line, the latter is a curved line slightly more accurate (Verdugo 1992) the equations adopted to define the CSL in the  $e:\log p'$  space are the following:

$$e = 1 - 0.2\ln(p') \quad (4)$$

$$e_v = 1 - 0.374 \left( \frac{p'}{p'_{ref}} \right)^{0.19} \quad (5)$$

where  $p'_{ref} = 100$  kPa.

Once the experimental parameters we determined, the calibration and validation of the NorSand model were done simulating each triaxial test using Visual Basic coding

with an open source code, written by Been and Jefferies (Jefferies and Been 2016) and this results were compared against the experimental ones (Fig. 2).

The following observations were done, remarkable agreement is obtained from the CIU tests, especially in terms  $p'$ - $q$  and  $q$ - $\varepsilon_a$ , but also as it is seen, the stress path that defines the CSL, for the CID tests, a good agreement with data is achieved, with limitations reproducing the behavior of volumetric strains and  $q$ - $\varepsilon_a$ . However, the relationship between axial and volumetric deformations shows a good adherence only until the peak deviator stress, after reaching this value, the experimental volumetric deformation is not reduced considerably and diverges from the model results where the deviator stress drops, this is seen in CIU tests (Fig. 3).

The divergence may be associated with the formation of shear bands and limitation of the boundary conditions defined in the modelling (Silva et al. 2022) also during the failure of the dense samples a rupture plane was well defined which is an experimental evidence of the shear band hypothesis, and the visual basic coding implements a single Cauchy stress tensor, so shear bands are not allowed in this implementation (Silva et al. 2022).

**Table 2.** NorSand Parameters

Pameter	
$\Gamma$	1
$\lambda_{10}$	0.2
$M_{tc}$	0.97
$N$	0
$\chi$	5
$H_0$	80
$H_\Psi$	500
$\nu$	0.2

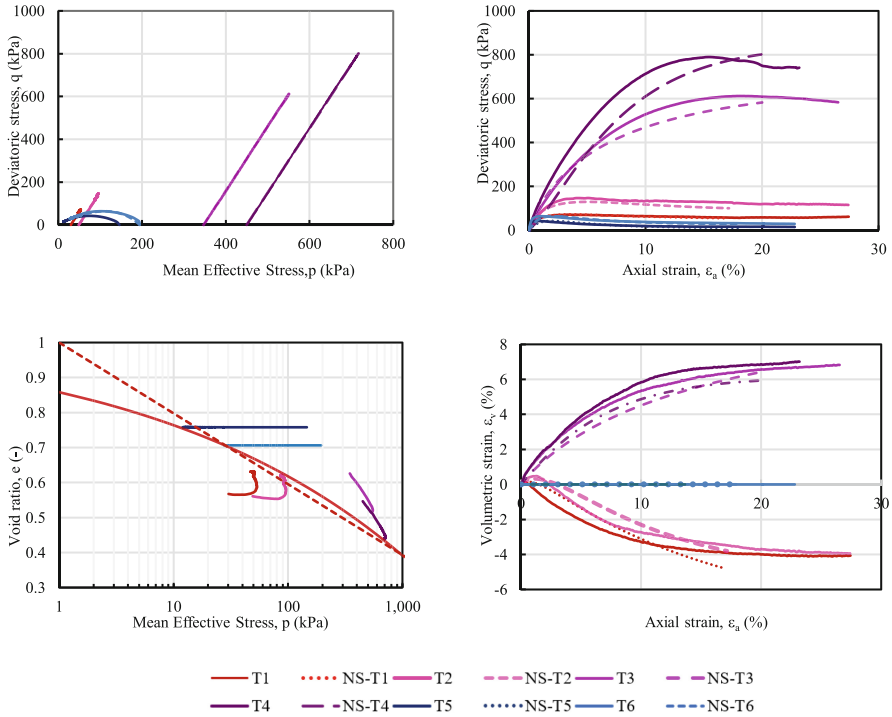


Fig. 3. Comparison between laboratory data and NorSand calibration

### 4 Conclusion

Characterization of silt-like mine tailings was presented to provide a description of the material and evaluate the predictive capacity of NorSand, a critical state model.

There was a consistent resemblance to the experimental results of drained and undrained tests and the simulations done using visual basic coding, nevertheless the volumetric deformation obtained during simulations presented a slightly divergence.

The full saturation conditions of soil specimens were achieved implementing the carbon dioxide method, water flushing and back pressure increment, along with the use of lubricated end platens provided a reliable characterization of CSL.

### References

Been, K., & Jefferies, M. (1985). A State Parameter for Sands. *Geotechnique*, 35, 99–112.  
 Castro, G. (1969). Liquefaction of Sands. *Harvard Soil Mechanics Series*.  
 Fonseca, A. V., Cordeiro, D., & Molina-Gómez, F. (2021). Recommended Procedures to Assess Critical State Locus from Triaxial Tests in Cohesionless Remoulded Samples. *Geotechnics*, 1(1), 95–127. <https://doi.org/10.3390/geotechnics1010006>.  
 Jefferies, M., & Been, K. (2016). *Soil liquefaction, a critical state approach* (CRC Press (ed.); 2nd ed.). Taylor & Francis Group.



- Nova, R. (1982). A constitutive model under monotonic and cyclic loading. In O. Zienkiewicz & G. Pande (Eds.), *Soil Mechanics – Transient and Cyclic Loads* (pp. 343–373). Wiley.
- Roscoe, K., Schofield, A., & Wroth, C. (1958). On the Yielding of Soils. *Geotechnique*, 8, 22–53.
- Rowe, P., & Barden, L. (1964). Importance of Free Ends in Triaxial Testing. *Soil Mechanics and Foundations, Proceedings of the American Society of Civil Engineers*.
- Seed, H., & Idriss, I. (1983). Evaluation of liquefaction potential using field performance data. *ASCE*, 109, 458–482.
- Silva, J. P. de S., Cacciari, P. P., Torres, V. F. N., Ribeiro, L. F. M., & de Assis, A. P. (2022). Behavioural analysis of iron ore tailings through critical state soil mechanics. *Soils and Rocks*, 45(2), 1–13. <https://doi.org/10.28927/SR.2022.071921>.
- U.S. Department of the Interior Bureau of Reclamation. (1999). Engineering Classification and Description of Soil. *USBR Engineering Geology Field Manual Volume 1*, 40.
- Verdugo, R. (1992). Discussion on “The critical state of sand.” *Geotechnique*, 42, 655–658.
- Woudstra, L. J. (2021). *Verification, Validation and Application of the NorSand Constitutive Model in PLAXIS*. Delft University of Technology.

**Open Access** This chapter is licensed under the terms of the Creative Commons Attribution-NonCommercial 4.0 International License (<http://creativecommons.org/licenses/by-nc/4.0/>), which permits any noncommercial use, sharing, adaptation, distribution and reproduction in any medium or format, as long as you give appropriate credit to the original author(s) and the source, provide a link to the Creative Commons license and indicate if changes were made.

The images or other third party material in this chapter are included in the chapter’s Creative Commons license, unless indicated otherwise in a credit line to the material. If material is not included in the chapter’s Creative Commons license and your intended use is not permitted by statutory regulation or exceeds the permitted use, you will need to obtain permission directly from the copyright holder.

